Available Online at http://www.journalajst.com

ASIAN JOURNAL OF SCIENCE AND TECHNOLOGY

ISSN: 0976-3376

Asian Journal of Science and Technology
Vol. 09, Issue, 01, pp.7398-7403, January, 2018

RESEARCH ARTICLE

CHARACTERIZATION AND PHOTOCATALYTIC PROPERTIES OF Cd-DOPED $Zn_3(VO_4)_2$ NANOPARTICLES SYNTHESIZED BY MICROWAVE COMBUSTION METHOD

***[1]Daisy Rani, J., [2]Lakshmi, D. and [3]Sundaram, R.**

[1]Department of Chemistry, Jeppiaar Engineering College, Chennai – 600 119, India
[2]Department of Plant Biology and Plant Biotechnology, Shrimathi Devkunvar Nanalal Bhatt Vaishnav College for Women, Chennai – 600 044, India
[3]Department of Chemistry, Presidency College, Chennai – 600 005, India

ARTICLE INFO

Article History:
Received 05th October, 2017
Received in revised form
15th November, 2017
Accepted 20th December, 2017
Published online 31st January, 2018

Key words:
$Zn_3(VO_4)_2$ nanoparticles,
Microwave combustion method,
Photocatalytic activity.

ABSTRACT

The $Zn_3(VO_4)_2$ nanoparticles doped with cadmium ions have been successfully synthesized by rapid microwave combustion method. The synthesized product was characterized by powder XRD, EDS, SEM, TEM, photoluminescence and VSM studies. XRD and EDS analyses suggest the effects of doping concentration on phase structures of $Zn_3(VO_4)_2$ nanoparticles. Photoluminescence emissions are centered at around 470 nm. Magnetic analysis revealed that the $Zn_3(VO_4)_2$ nanoparticles had a ferromagnetic behavior at room temperature with saturation magnetization of 18.23 emu/g. The results of the photocatalytic degradation of methyl orange in aqueous solution showed that cadmium ions doping greatly improved the photocatalytic efficiency of $Zn_3(VO_4)_2$ nanoparticles. The Cd-doped $Zn_3(VO_4)_2$ nanoparticles with atomic ratio of Cd to Zn being 0.08 had the best activity in photo-degradation of methyl orange in aqueous solution under UV light irradiation.

INTRODUCTION

In the last two decades, photo catalysis in the presence of semiconductors caused a wide range of concern because it can be used in environmental protection (Pan, 2013). Among these semiconductors vanadate is well-known as an excellent candidate for photocatalytic reaction owing to its high photocatalytic activity, environmental compatible feature and relatively low cost (Nalwa, 2004). Transition metal vanadates are studied extensively in recent years due to their fascinating structures, electronic, optical, magnetic and photocatalytic properties. Dyes are important organic pollutants, and their release as waste water in the ecosystem is a dramatic source of esthetic pollution, eutrophication, and perturbations in aquatic life (Fu, 2005). Photocatalytic degradation of organic compounds for the purpose of purifying waste water from industries has attracted much attention in recent years (Arularasu, 2017; Kamat, 2002 and Yu, 2007). TiO_2 has been dominantly used because of its high activity, long-term stability, low price, and availability. However, TiO_2 is a wide band gap semiconductor, which necessitates the use of mainly ultraviolet irradiation (Kazuya Nakata, 2012). The solar spectrum usually contains about 4% UV light. Thus, exploitation of a new photo catalyst system is compulsory. Recently, a growing interest was also focused on the non-TiO_2-based catalyzers.

****Corresponding author:*** **Daisy Rani, J.,**
Department of Chemistry, Jeppiaar Engineering College, Chennai – 600 119, India

Many different semiconductors, such as, V_2O_5, WO_3, ZnO, Fe_2O_3, CdO and CdS, have been used as photo catalysts for the photo degradation of organic or inorganic pollutants (Arularasu, 2017; Bamwenda, 2001; Sathish, 2007). However, there were only a few reports about vanadium based heterogeneous photo catalysts, such as $Zn_3(VO_4)_2$, CdV_2O_6, Bi_2VO_6 (Tokunaga, 2002; Liang, 2012; Kohtani, 2005). $Zn_3(VO_4)_2$ and CdV_2O_6 were reported to be good photo catalysts for photo-degradation of organic compounds under UV light irradiation. These results suggest the vanadium-based photo catalysts may have potential application in environmental purification. In the past decade, $Zn_3(VO_4)_2$ has attracted much attention because of its magnetic, scintillated, luminescent and catalytic properties (Min, 2011 and Pitale,, 2012). The preparation of nanostructures with controlled size, morphology and composition of the materials are of great interest, because of their unique physical and chemical properties. It is well-known that nanometer-sized inorganic low-dimensional systems exhibit a wide range of optical and catalytic properties that rely sensitively on both size and morphology. The photocatalytic activity of catalysts depended strongly on two factors: adsorption behavior and the separation efficiency of electron–hole pairs. The adsorption capacity can be generally improved by increasing the specific surface area of catalysts. On the other hand, in order to eliminate the recombination rate of the electron–hole pairs, metal ions doping have been proposed (Hoffmann, 1995 and Xie, 2005). In this present study, $Zn_3(VO_4)_2$ nanoparticles were

synthesized by a microwave combustion method. However, microwave combustion method has more advantages than other methods, such as simple process, low cost and high purity products. Therefore, microwave combustion method is a very popular synthesis method to synthesize photo catalysts and plays key role in tailoring the properties of nanomaterials due to its potential controllability over size and morphology (Shi, 2003). Recently Cu-Ni bimetallic nanoalloys have also been prepared by a rapid microwave combustion method (Arul Mary, 2014). Hence, we report the synthesis of Cd-doped $Zn_3(VO_4)_2$ nanoparticles by the microwave combustion method. The photocatalytic activities of the as prepared samples for the methyl orange (MO) photo-degradation were investigated. To further understand the mechanism of Cd doped $Zn_3(VO_4)_2$ nanoparticles, photo catalysis, the effects of preparation conditions and Cd-doping concentrations on the photocatalytic activity were discussed.

Experimental Techniques

Fabrication of Cd doped $Zn_3(VO_4)_2$ nanoparticles: All the chemicals were analytic grade reagents without further purification. Cd-doped $Zn_3(VO_4)_2$ nanoparticles were synthesized by rapid microwave combustion method. $ZnCl_2$ (0.306g) was dissolved in 15 ml distilled water and $CdCl_2 \cdot 2.5H_2O$ (the atomic ratios of Cd to Zn being 0, 0.02, 0.04, 0.06, 0.08, respectively) was added to it with vigorous stirring. NH_4VO_3 (0.175g) was dissolved in 30 ml of hot double distilled water and slowly drop wise mixed to the above solution under continuous stirring, and the pH of the solution was adjusted to 9, with 1 M HCl solution. The resulting suspension was placed in a domestic microwave oven and exposed to the microwave energy in a 2.45 GHz multimode cavity at 850 W for 10 min. Initially, the precursor mixture boiled and underwent evaporation followed by the decomposition with the evolution of gases. When the solution reached the point of spontaneous combustion, it vaporized and instantly became a solid. For convenience of description, changing the atomic ratio of Cd to Zn, the 0.00, 0.02, 0.04, 0.06 and 0.08 doping of cadmium ions in $Zn_3(VO_4)_2$ nanoparticles were marked as A, B, C, D and E, respectively.

Characterization of $Zn_3(VO_4)_2$ nanoparticles

The X-ray diffraction (XRD, Thermo ARL SCINTAG X'TRA with Cu Ka irradiation, λ = 0.1540 nm) was used to analyze the crystalline size and purity of the samples. The composition of the product was analyzed by energy dispersive X-ray detector (EDS, Thermo Noran VANTAG-ESI). The morphologies were characterized using scanning electron microscopy (SEM, Hitachi S-4800, 25 kV) and transmission electron microscopy (TEM, JEM200CX, 120 kV). The composition of the product was analyzed by energy dispersive X-ray detector (EDS, Thermo Noran VANTAG-ESI). BET surface areas were measured by nitrogen adsorption at 77K using a Micromeritics ASAP 2000 surface area analyzer. Photoluminescence spectrum of the samples was recorded on a Edinburgh FL/FS TCSPC 920 fluorescence spectrometer. Magnetic measurements were carried out at room temperature using a PMC MicroMag 3900 model vibrating sample magnetometer (VSM) equipped with 1 T magnet.

Photocatalytic experiments: The photo activity experiments on the samples for the photo degradation of methyl orange were performed at ambient temperature. Ultraviolet source was a 12W Hg lamp (λ = 254 nm, Institute of Electric Light Source, Beijing). In a typical process, aqueous suspension of methyl orange (150 mL, $C_0 = 1\times10^{-5}$ M) and 50 mg of Cd-doped $Zn_3(VO_4)_2$ nanoparticles were placed in a vessel. Prior to irradiation, the suspension was magnetically stirred in the dark for ca. 30 min to ensure the equilibrium of the working solution. The suspension had been kept under constant air-equilibrated conditions before and during the irradiation. pH of the reaction suspension has been not adjusted. Analytical samples (4 mL) were drawn from the reaction suspension every 5 min, and removal of Cd-doped $Zn_3(VO_4)_2$ nanoparticles by centrifugation. The change of absorption at wavelength 550 nm was applied to identify the concentration of methyl orange using a 721-type spectrophotometer. The percentage of degradation is reported as C/C_0. C is the maximum peak of the absorption spectra of methyl orange for each irradiated time interval at 550 nm. C_0 is the absorption of the starting concentration when adsorption/desorption equilibrium was achieved. To test its photocatalytic lifetime, Cd-doped $Zn_3(VO_4)_2$ nanoparticles were recycled and reused five times in the decomposition of methyl orange under the same conditions. After each photocatalytic reaction, the aqueous solution was centrifuged to recycle Cd-doped $Zn_3(VO_4)_2$ nanoparticles that were then dried at 100^0C for another test.

RESULTS AND DISCUSSION

The phase structure and the phase composition of the $Zn_3(VO_4)_2$ nanoparticles were examined by XRD and EDS. Fig. 1 shows the effects of Cd-doping concentration on phase structures of the $Zn_3(VO_4)_2$ nanoparticles prepared by microwave combustion method. All the main peaks can be indexed undisputedly as the pure phase of monoclinic wolframite (space group: P2/c), which was in good agreement with the standard data (JCPDS card no. 034-0378) (Pitale, 2012). The cadmium ions may be easy to insert into the structure of $Zn_3(VO_4)_2$ nanoparticles, due to $Zn_3(VO_4)_2$ and $CdVO_4$ with the same crystal structure. The average crystallite size was calculated using Scherrer's formula given in below.

$$D = 0.89\lambda/\beta\cos\theta$$

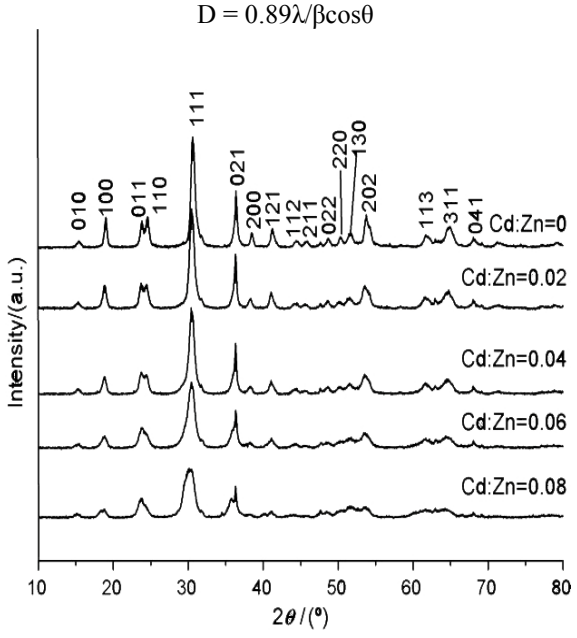

Figure 1. XRD patterns of the $Zn_3(VO_4)_2$ nanoparticles prepared at different Cd-doping concentration. (a) 0 %, (b) 0.02 %, (c) 0.04 %, (d) 0.06 % & (e) 0.08 %

Where D is the crystallite size; λ is the X-ray wavelength; β is the full width at half maximum (FWHM); θ is the Bragg diffraction angle. The average crystallite size D calculated from the diffraction peaks was found to be 21.56^o – 33.25^o nm for $Zn_3(VO_4)_2$ nanoparticles. Energy dispersive spectrometry (EDS) analysis was employed to determine the composition of the Cd-doped $Zn_3(VO_4)_2$ nanoparticles.

The EDS patterns of the $Zn_3(VO_4)_2$ nanoparticles doped with different contents of cadmium ions are shown in Fig. 2. With Cd-doping concentration increasing, the Cd peak intensity slightly increased. The results from EDS confirm that the obtained products are composed of the $Zn_3(VO_4)_2$ nanoparticles doped with cadmium ions. The four major peaks corresponded to vanadium, zinc, oxygen, and cadmium, respectively.

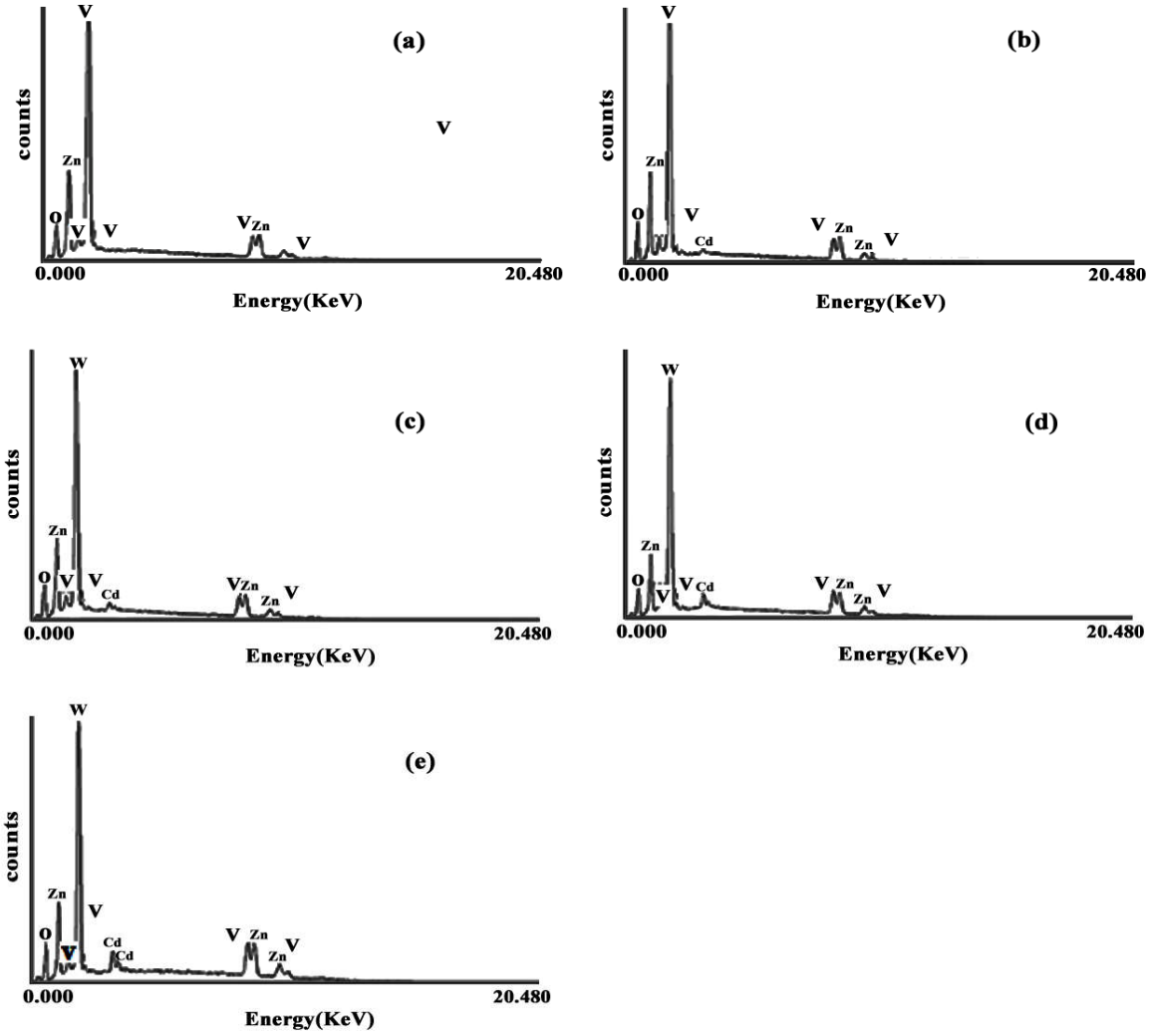

Figure 2. EDS of the $Zn_3(VO_4)_2$ nanoparticles prepared at different Cd-doping concentration. (a) 0%, (b) 0.02 %, (c) 0.04 %, (d) 0.06 % & (e) 0.08 %

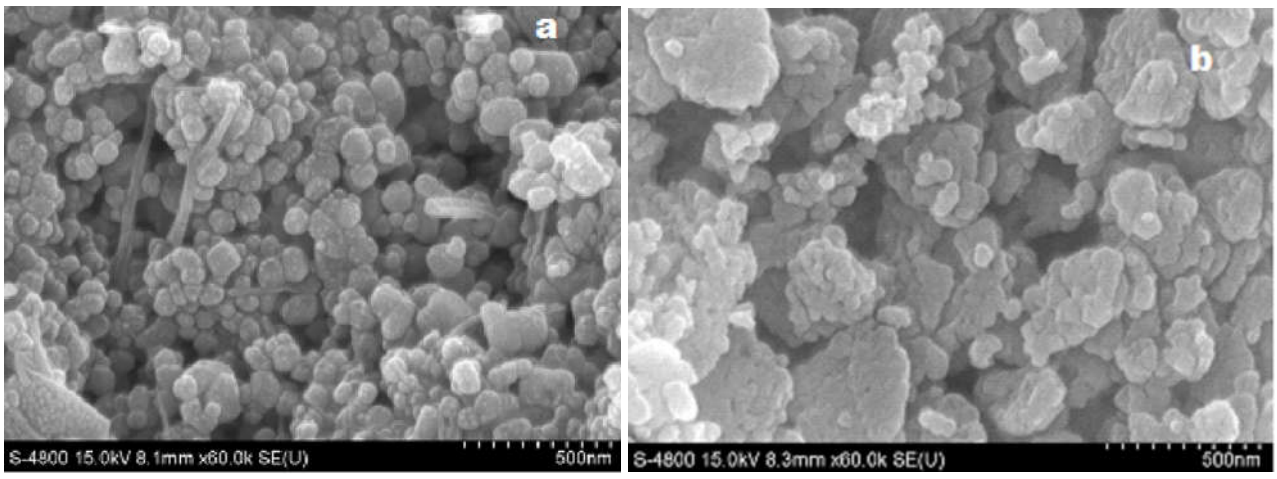

Figure 3. SEM images of the $Zn_3(VO_4)_2$ nanoparticles (a) 0 % (b) 0.08 % doped

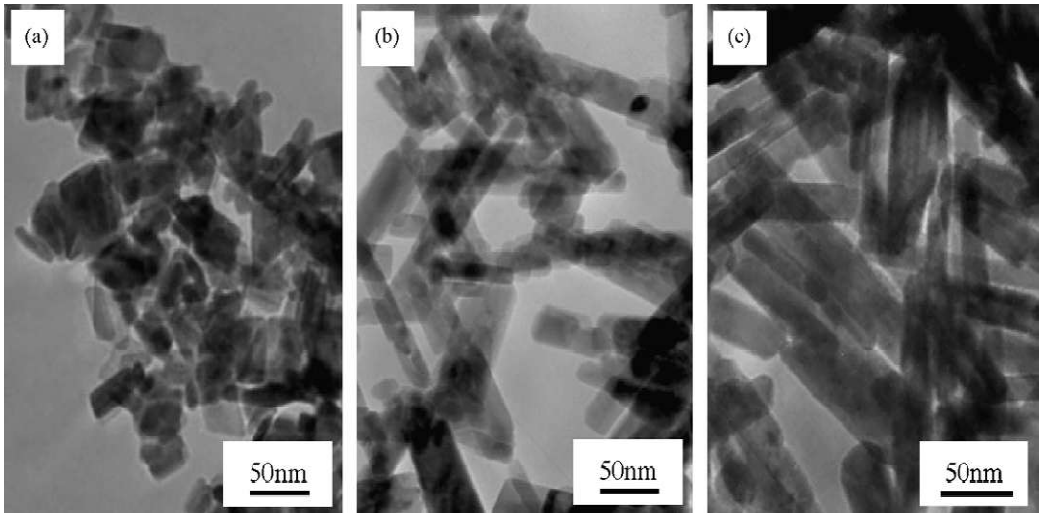

Figure 4. TEM images of the $Zn_3(VO_4)_2$ nanoparticles (a) 0 % (b) 0.06 % (c) 0.08 %

Table 1. BET surface area of the samples prepared at the different Cd-doping concentrations

Cd-doping concentration	0	0.02	0.04	0.06	0.08
Surface area (m^2 g^{-1})	35.4	35.9	36.2	36.4	36.9

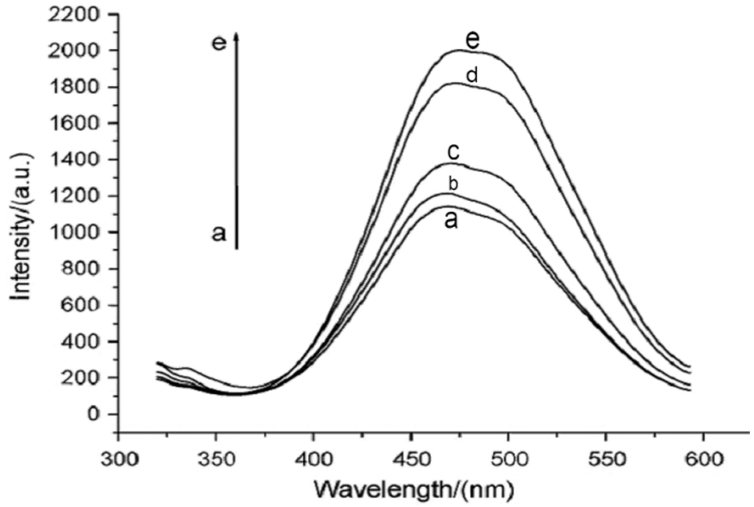

Figure 5. PL spectra of the $Zn_3(VO_4)_2$ nanoparticles doped with different contents of cadmium ion. From (a–e), the doping ratio of Cd/Zn was 0, 0.02, 0.04, 0.06 and 0.08

The morphology and particle sizes of the samples were investigated by SEM and TEM. The SEM image of Cd-doped $Zn_3(VO_4)_2$ nanoparticles in Fig. 3 further demonstrates that the obtained product has a uniform rod like morphology. Fig. 4 shows the TEM image of pure $Zn_3(VO_4)_2$ nanoparticles prepared via microwave combustion method. As can be seen from the TEM images of samples prepared at different Cd-doping concentration, Cd-doped $Zn_3(VO_4)_2$ nanoparticles can be obtained in the whole concentration range under investigation (Cd/Zn: 0.02–0.08), which indicates that the Cd-doping concentration has little effect on the crystal morphology in this range. The size of the nanoparticles was consistent with TEM results. BET surface area of the samples prepared at the different Cd doping concentration is shown in Table 1. It can be observed that the presence of different amounts of Cd species on the $Zn_3(VO_4)_2$ nanoparticles surface does not influence significantly the value of the BET surface area of $Zn_3(VO_4)_2$ nanoparticles. This indicates that specific surface area of the sample is not consequentially in association with the photocatalytic activity. Fig. 5 shows the room temperature PL emissions of the $Zn_3(VO_4)_2$ nanoparticles doped with different contents of cadmium ions. The luminescence spectra of the Cd-doped $Zn_3(VO_4)_2$ nanoparticles exhibit broad blue–green emission bands peaking at 467nm with a shoulder at 494 nm. It can be seen that the Cd dopant does not result in new PL phenomena. However, the excitonic PL intensity of the $Zn_3(VO_4)_2$ nanoparticles increases as the increasing of cadmium ion content. It is known that the excitonic PL of semiconductor nanoparticles mainly results from surface oxygen vacancies and defects. Thus, during the dopant system, the excitonic PL spectrum is stronger, the content of surface oxygen vacancy and defect is higher. When the dopant content is lower than its optimal ratio (Cd/Zn = 0.08), according to Figs. 5 and 6, it can be found that the excitonic PL spectra is stronger, the photocatalytic activity is higher.

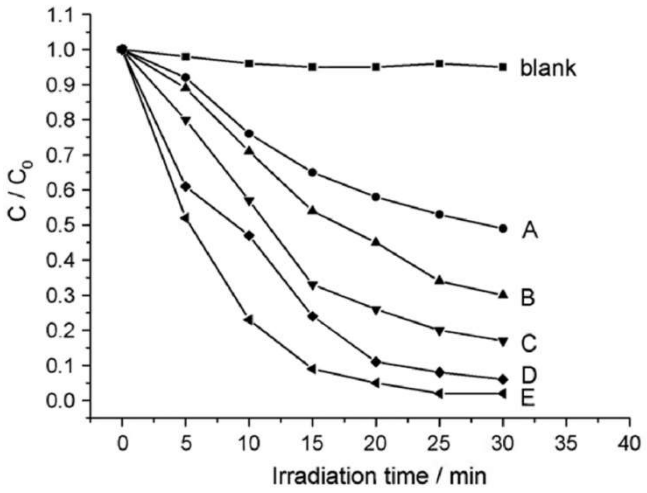

Figure 6. Photocatalytic degradation of methyl orange by the $Zn_3(VO_4)_2$ nanoparticles prepared at different Cd-doping concentration

Fig. 6 shows the photocatalytic degradation rates of methyl orange on Cd-doped $Zn_3(VO_4)_2$ nanoparticles with different cadmium contents. The sample E has the highest photocatalytic activity, and the conversion of methyl orange can be nearly up to 100% after 30 min of irradiation. The blank experiment without catalyst shows that methyl orange is almost not decomposed under the same irradiation time, indicating that the Cd-doped $Zn_3(VO_4)_2$ photo catalyst leads to the photo-degradation of methyl orange, when Cd-doping concentration is lower than 0.08, Fig. 6 shows that the degradation rate increases as the increase of cadmium ion content. However, if Cd-doping concentration further increases, the photocatalytic activity decreases obviously. During the process of photocatalytic reaction, oxygen vacancies and defects can become center to capture photo-induced electrons, so that the recombination of photo-induced electrons and holes can be effectively inhibited. When the dopant content is more than its optimal value, the oxygen vacancies and defects will be a recombination center. According to the above discussion, the presence of a small amount of cadmium ion can enhance the activity, but excessive cadmium ion is detrimental. This may be due to the fact that the cadmium ion can serve as a mediator of the transfer of interfacial charge at an appropriate doping concentration, and a small amount of cadmium ion acting as a photo-generated hole and a photo-generated electron trap inhibits the hole–electron recombination.

The stability of Cd-doped $Zn_3(VO_4)_2$ nanoparticles (E) was investigated due to its importance in application. After five recycles for the photo-degradation of methyl orange (Fig. 7), the catalyst did not exhibit any significant loss of activity, confirming that Cd-doped $Zn_3(VO_4)_2$ nanoparticles (E) is not photo corroded during the photocatalytic oxidation of the pollutant molecules. Magnetic proportions of the sample E were carried out at room temperature in order to Envisage their behavior of magnetic state. The VSM measurement recorded in the range of -15k0e to +15kOe applied magnetic field. Fig. 8 show the sample E, magnetic behavior by a typical hysteresis loop. The value of remnant magnetization (Mr) is 2.45 emu/g and the saturation magnetization (Ms) value around 18.23 emu/g. The coercivity field around 17.75 Oe, this value represent the synthesized sample E have ferromagnetic property. From the slender hysteresis curve suggests ferromagnetism due to uncompensated spins are present in the sublattice (Arularasu, 2016).

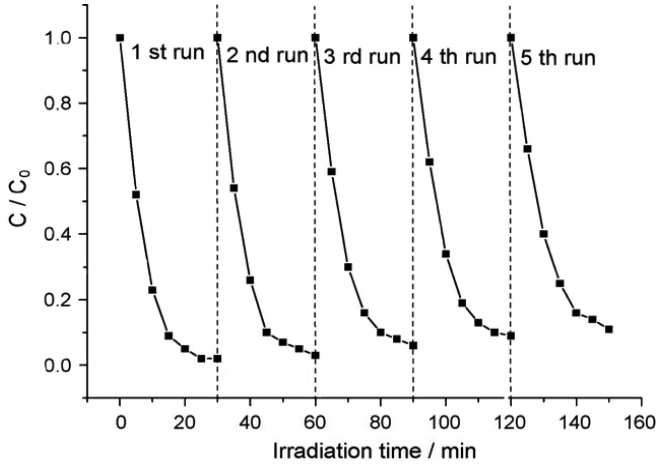

Figure 7. The lifetime for photo-degradation of methyl orange by 0.08 % doped $Zn_3(VO_4)_2$

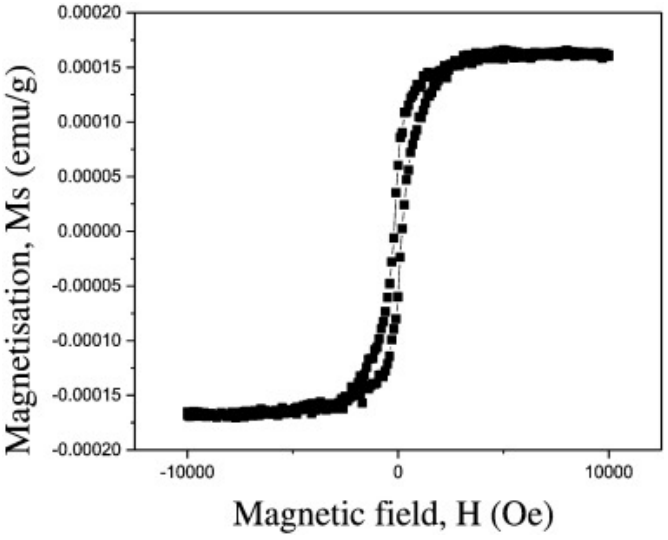

Figure 8. VSM studies of sample 0.08 % Cd doped $Zn_3(VO_4)_2$

Conclusion

The Cd-doped $Zn_3(VO_4)_2$ nanoparticles were successfully prepared by a microwave combustion method and it exhibited the high photocatalytic activity for the decomposition of the aqueous methyl orange. Synthesized sample E shows a ferromagnetic property. A small amount of Cd-doping could obviously enhance the photocatalytic activity of $Zn_3(VO_4)_2$ nanoparticles. At an optimal atomic ratio of Cd to Zn of 0.08, sample has the highest photocatalytic activity, and the conversion of methyl orange can be nearly up to 100% after 30 min of irradiation. The high activity of the Cd-doped $Zn_3(VO_4)_2$ nanoparticles could be attributed to the synergetic effects of Cd-doping and crystallinity structure. The mechanism for the photo-degradation performance needs to be further researched.

Acknowledgements

The authors are thankful to the management of Jeppiaar Engineering College and SDNB Vaishnav College for women, Chennai for providing necessary lab facilities.

REFERENCES

Arul Mary, J., Manikandan, A., John Kennedy, L. Bououdina, M., Sundaram, R., Judith Vijaya, J. 2014. Structure and magnetic properties of Cu−Ni alloy nanoparticles prepared by rapid microwave combustion method, *Trans. Nonferrous. Met.Soc. China*., 24, pp.1467-1473.

Arularasu, M. V., Anbarasu, M., Poovaragan, S., Sundaram, R., Kanimozhi, K., Maria Magdalane, C., Kaviyarasu, K. Thema, F. T., Letsholathebe, D., Genene T. Mola, M. Maaza, 2017. Structural, optical, morphological and microbial studies on SnO_2 nanoparticles prepared by co-precipitation method, *Journal of Nanoscience and Nanotechnology,*17,1-7.

Arularasu, M.V., Sundaram, R. 2016. Synthesis and characterization of nanocrystalline $ZnWO_4$-ZnO composites and humidity sensing performance*, Sensing and Bio-Sensing Research*, 11, 20–25

Arularasu, M. V., Anbarasu, M., Poovaragan, S., Sundaram, R., Kanimozhi, K., Maria Magdalane, C., Kaviyarasu, K., Thema, F.T., Letsholathebe, D., Genene T. Mola, M. Maaza, 2017. Synthesis, humidity sensing, photocatalytic and antimicrobial properties of thin film nanoporous $PbWO_4$-WO_3 Nanocomposites, *Journal of Nanostructures,* 7,1,pp.47-56.

Bamwenda, G.R. and Arakawa, H. 2001. The visible light induced photocatalytic activity of tungsten trioxide powders, *Appl. Catal*. A, 210, pp. 181-191.

Chen, C.C. 2007. Degradation pathways of ethyl violet by photocatalytic reaction with ZnO dispersions, *J. Mol. Catal*. A, 264, pp. 82-92.

Fu, H., Pan, C., Yao, W. and Zhu, Y. 2005. Visible-Light-Induced Degradation of Rhodamine B by Nanosized Bi_2WO_6, *J. Phys. Chem*., B 109, pp. 22432-22439.

Hoffmann, M. R., Choi, S. T., Martin, W., Bahnemann, D. W. 1995. Environmental applications of semiconductor Photocatalysis, *Chem. Rev*., 95, pp. 69-96.

Kamat, P.V., Huehn., R. and Nicolaescu, R. 2002. A "Sense and Shoot" Approach for photocatalytic degradation of organic dontaminants in water, *J. Phys. Chem*. B., 106, pp. 788-794.

Kazuya Nakata, Akira Fujishima,2012. TiO_2 photocatalysis: Design and applications, *Journal of Photochemistry and Photobiology C: Photochemistry Reviews*, 13, 3, pp. 169-189. Ln^{n+}-TiO_2 sol in aqueous solution under visible light irradiation, *Mater. Sci. Eng*., B, 117, pp.325-333.

Kohtani, S., Tomohiro, M., Tokumura, K. and Nakagak, R. 2005. Photo oxidation reactions of polycyclic aromatic hydrocarbons over pure and Ag-loaded $BiVO_4$ photo catalysts, *Appl. Catal. B. Environ*., 58, pp. 265-272.

Liang, Y., Liu, P., Li, B. and Yang, G. W. 2012. Synthesis and characterization of copper vanadate nanostructures via electrochemistry assisted laser ablation in liquid and the optical multi-absorptions performance, *Cryst. Eng. Comm*., 14, pp. 3291-3296.

Liu, Y., Zhang, Y.C. and Xu, X.F. 2009. Hydrothermal synthesis and photocatalytic activity of CdO_2 nanocrystals *J. Hazard. Mater*., 163, pp. 1310-1314.

Min, W., Qiong, L. and Haiyan, L. 2011. Preparation, characterization and photocatalytic property of $BiVO_4$ Photocatalyst by Sol-gel Method, *Appl. Mech. Mater*., 99, pp. 1307-1311.

Nalwa H. S., (Ed.), 2004. *Encyclopedia of Nanoscience and Nanotechnology,* 1-10*,* American Scientific Publishers, Los Angeles, CA.

Pan, C. Ding, R. Hu, Y. C. Yang, G. J. 2013. Electrospinning fabrication of rime-like NiO nanowires/nanofibers hierarchical architecture sand their photocatalytic properties, *Physica E*, 54, pp. 138-142.

Pitale, S. S., Gohain, M., Nagpure, I. M. Ntwaeaborwa, O. M. Bezuidenhoudt, B.C.B., Swart, H.C. 2012. A comparative study on structural ,morphological and luminescencec characteristics of $Zn_3(VO_4)_2$ phosphor prepared via hydrothermal and citrate-gel combustion routes, *Physica B*, 407, pp.1485-1488.

Sathish, M. and Viswanath, R.P. 2007. Photocatalytic generation of hydrogen over mesoporous CdS nanoparticle: Effect of particle size, noble metal and support, *Catal. Today*, 129, pp. 421-427.

Shim, S. and Hwang, J.Y. 2003. Microwave-assisted wet chemical synthesis: advantages, significance, and steps to industrialization. *J. Min. Mat. Char. Eng*, 2, pp.101-110.

Tokunaga, S., Kato, H., Kuto, A. 2001. Selective Preparation of monoclinic and tetragonal $BiVO_4$ with Scheelite Structure and Their Photocatalytic Properties, *Chem. Mater*., 13, pp. 4624-4628.

Xie, Y. Yuan, C. and Li, X. 2005. Photosensitized and photocatalyzed degradation of azo dye using

Yu, J., Yu, X., Huang, B., Zhang, X. and Dai, Y. 2009. Hydrothermal Synthesis and Visible-light Photocatalytic Activity of Novel Cage-like Ferric Oxide Hollow Spheres, *Cryst. Growth Des*., 9, pp. 1474-1480.

Yu, J.G., Zhang, L.J., Cheng B., and Su, Y.R. 2007. Hydrothermal preparation and photocatalytic activity of hierarchically sponge-like macro/mesoporous titania, *J. Phys. Chem*., C, 111, 10582-10589.

****